



# Field emission properties of vertically aligned carbon nanotubes grown on bias-enhanced hydrogen plasma-pretreated Cr film

Chia-Fu Chen, Chien-Liang Lin\*, Chi-Ming Wang

Department of Materials Science and Engineering, National Chiao Tung University, 1001 Ta Hsueh Road, Hsinchu 30050, CA 92866, Taiwan, ROC

Received 12 December 2002; received in revised form 15 April 2003; accepted 10 July 2003

## Abstract

Using  $\text{CH}_4/\text{H}_2$  source gases, vertically aligned carbon nanotubes were grown on a Cr film by microwave plasma chemical vapor deposition. The Cr film on a silicon wafer had a constant thickness of 100 nm, and bias-enhanced  $\text{H}_2$  plasma pre-treatment was performed for various periods to modify the surface of the Cr film. Bias voltage of  $-150$  V was applied during both pre-treatment and growth steps, the resultant carbon nanotubes on a Cr film, which had been pretreated in bias-enhanced  $\text{H}_2$  plasma for 5 min were vertically aligned. The field emission properties of the resultant carbon nanotubes included an emission current of  $0.305$  mA at  $2$  V/ $\mu\text{m}$ ; and a turn-on field of  $1.7$  V/ $\mu\text{m}$ .

© 2003 Elsevier B.V. All rights reserved.

**Keywords:** Carbon; Chemical vapor deposition; Chromium; Field emission

## 1. Introduction

Field emission display is evolving as a promising technique for manufacturing the next generation of flat panel displays. Recently, field emission and vacuum microelectronic devices based on carbon nanotubes (CNTs) have exhibited remarkable emission characteristics and good current stability [1,2], attributable to the high-aspect-ratio, the electrical conductivity and the mechanical stiffness of the nanotubes [3,4].

Since carbon nanotubes were first observed by Iijima [5] in 1991, several approaches have been reported for growing CNTs in situ without pre-depositing a catalyst layer. One such method uses a reactant gas that can act as a catalyst for growing CNTs on certain substrates [6]. Moreover, the power of the plasma may promote the generation of small metal particles from the metal substrate in a plasma-enhanced chemical vapor deposition [7]. Accordingly, the authors believe that CNTs grow due to a particular effect of a reactant gas on the surface condition of substrates and these substrates have no way to provide proper catalytic particles for growing

CNTs originally unless their surface is modified before or during the CNTs growth. Therefore, this work develops vertically aligned CNTs (VACNTs) grown on bias-enhanced hydrogen plasma-pretreated Cr films using microwave plasma chemical vapor deposition and applies them to field emission. The Cr film was selected because it adheres well to silicon wafers and it is also a transition metal. Bias-enhanced  $\text{H}_2$  plasma pre-treatment was performed for various periods to modify the surface conditions of the Cr film. Varying the pre-treatment periods between 1 min and 30 min was found to form catalytic particles of different sizes. The size of the catalytic particles in turn determines the growth of VACNTs.

## 2. Experimental aspects

CNTs were deposited using microwave plasma chemical vapor deposition. The Cr film on a silicon wafer had a constant thickness of 100 nm and was coated on by DC sputtering. Before deposition, samples were sonicated in acetone for 10 min, washed with DI water and dried using nitrogen gas. Bias-enhanced  $\text{H}_2$  plasma pre-treatment was performed for various periods to modify the surface of the Cr film. The applied micro-

\*Corresponding author. Tel.: +886-955979496; fax: +886-35504502.

E-mail address: [u8818806@cc.nctu.edu.tw](mailto:u8818806@cc.nctu.edu.tw) (C.-L. Lin).

wave power and the working pressure were 400 W and 2666 Pa, respectively. During the Cr film pre-treatment with H<sub>2</sub> plasma, the flow rate of H<sub>2</sub> was maintained at 300 sccm, and the negative bias voltage applied to the substrates was –150 V. During the growth of CNTs, microwave power, negative bias and working pressure were not changed. The reactive gas mixture was CH<sub>4</sub>/H<sub>2</sub> at a flow rate of 30/270 sccm. An optical pyrometer was used to monitor the substrate temperature, which was maintained at approximately 700 °C. In each case, growth continued for 30 min beyond the period of pre-treatment.

A scanning electron microscope (SEM) (S-4000, Hitachi) was used to observe the morphology of the pretreated Cr films and their growing samples. The surface roughness, average grain size and particle size of the pretreated Cr film were determined using an atomic force microscope (AFM) (NanoScope, Digital Instruments). A Renishaw micro-Raman spectroscopy with an argon ion laser (514.5 nm line) was used to characterize the quality of the growing samples. The *I*–*V* measurements using a diode structure were used to analyze the field emission properties of the CNTs. Finally, the nanotubes were scratched off from the specific sample and sonicated in acetone for 10 min before being dropped on a hole carbon copper grid, and imaged using a transmission electron microscope (TEM) (Tecnai 20, Philips), to further characterize their structure.

### 3. Results and discussion

In this study, the deposition of CNTs proceeded in two steps: the pre-treatment of Cr film with bias-enhanced H<sub>2</sub> plasma and the growth of CNTs. The Cr surface was expected to be treated effectively by high capacity for etching. Thus, pre-treatment was performed under bias to reduce the period over which the surface was modified. The resulting samples were examined by sampling and they did not differ according to the condition, whether they underwent pre-treatment and growth simultaneously or separately.

#### 3.1. Bias-enhanced H<sub>2</sub> plasma pre-treatment of Cr film

Fig. 1 shows the SEM photographs of Cr films pretreated with H<sub>2</sub> plasma for various periods. The surface of the silicon wafer, which was originally covered by a Cr film, appeared after 10 min, and etching seemed more severe after 30 min, as shown in Fig. 1e,f. The hydrogen plasma has been used as an etching source in many applications. Thus, in this work, the accelerated active hydrogen radicals under bias yield anisotropic etching. However, this high capacity for etching may be appreciated even during short pre-treatment. Unlike for the as-deposited Cr film sample,

shown in Fig. 1a, pre-treatment periods between 1 and 5 min, Fig. 1b–d resulted in obvious surface changes.

The surface roughness, average grain size and particle size of pretreated Cr films were analyzed by AFM. Fig. 2 shows the surface roughness, average grain size and particle size of Cr films for various periods of treatment with H<sub>2</sub> plasma. Longer pre-treatment resulted in rougher surfaces and larger particles on the Cr film. The surface roughness, average grain size and particle size of a particular Cr film when growing CNTs were 26.871 nm, 928.74 nm<sup>2</sup> and 80.409 nm, respectively. These obtained analytic results, which shows the particle size to be the major factor that affects the growth of CNTs. CNTs were experimentally demonstrated to grow by precipitation of carbon from supersaturated transition metal particles and the diameter of CNTs was closely correlated with the size of dispersed metal particles [8,9]. However, the diffusion model for the growth of CNTs does not have universal significance and growth conditions can also significantly affect the formation of CNTs [10].

#### 3.2. Growth of VACNTs

Fig. 3 shows SEM photographs of samples grown on H<sub>2</sub> plasma-pretreated Cr film pretreated for various periods. As shown in Fig. 3a, no nanotube was found on the surface of a Cr film pretreated with H<sub>2</sub> plasma for 3 min. The VACNTs seem only to have grown on the surface of Cr films pretreated with H<sub>2</sub> plasma-pretreated for 5 min or 10 min, as shown in Fig. 3b and c, respectively. These CNTs possess a high-aspect-ratio, implying potential use as field emission devices.

The first-order Raman spectrum of the CNTs includes strong, sharp peaks at 1581 cm<sup>-1</sup> (G-line) and 1350 cm<sup>-1</sup> (D-line). The peaks suggest that the CNTs are characteristic of microcrystalline graphite. Fig. 4 displays the Raman spectra of the carbon grown on Cr film with various periods of pre-treatment. As shown in Fig. 4a,b only samples pretreated for 3 and 5 min showed two peaks at approximately 1350 and 1581 cm<sup>-1</sup>. The relative intensities of the two peaks depend on the type of graphitic material. Normally, the intensity of the 1350 cm<sup>-1</sup> peak increases as (i) the amount of disorganized carbon in the samples increases or (ii) the graphite crystal size decreases. However, the SEM photograph in Fig. 3a shows that no CNT grew on the sample with 3 min of H<sub>2</sub> pre-treatment, the peaks seem to be associated with amorphous carbon since both resemble those in the Raman spectrum. Furthermore, as shown in Fig. 4c, the Raman spectrum indicates that the sample with 10 min of H<sub>2</sub> pre-treatment did not include carbon, which fact is interesting, since this sample looks like carbon tips as shown in Fig. 3c. After further characterized by X-ray diffraction, this sample was verified to be silicon. This maybe due to the surface of

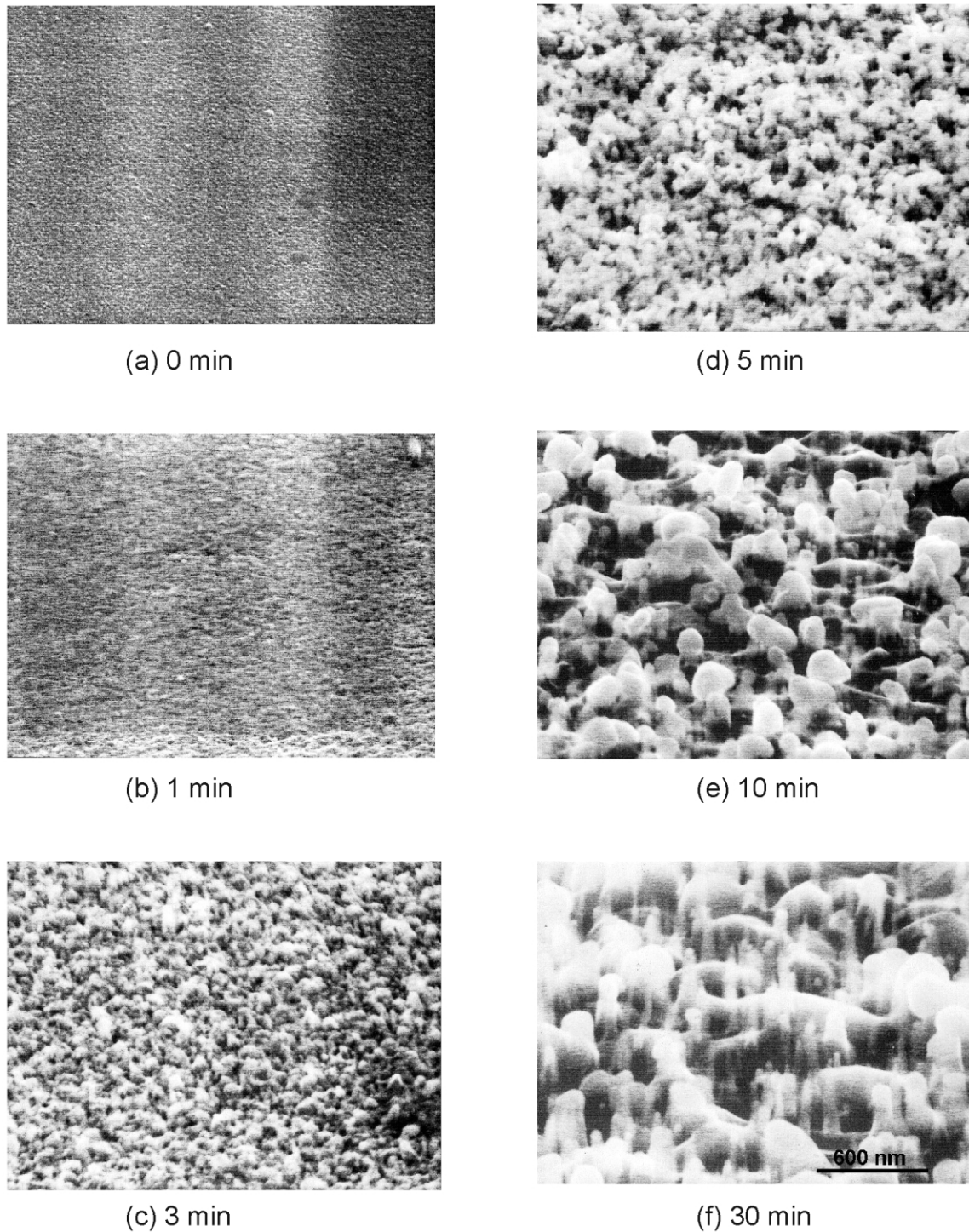


Fig. 1. SEM photographs of bias-enhanced  $H_2$  plasma-pretreated Cr film, obtained for various periods of pre-treatment.

the silicon wafer appeared after pre-treatment. While in the growth step, lacking for the protection of Cr and the proper catalysts, the silicon sample suffered a more severe anisotropic etching.

The CNTs were analyzed by TEM to confirm that they were truly CNTs, and not carbon fibers. Fig. 5 displays the TEM image of an end section of an

individual CNT. Comparing this image to those presented elsewhere, [8] indicates that the tube is a multi-walled CNT. The darkness of the nanotube walls indicates that the nanotube is multi-walled and hollow rather than solid fibers. Fig. 5 also reveals that the CNT has inner diameters of approximately 10 nm and outer diameters of approximately 30 nm. The Cr was also

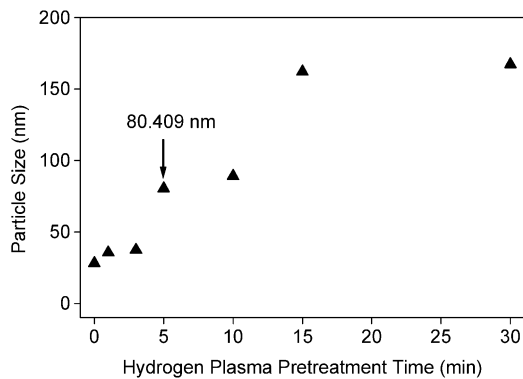
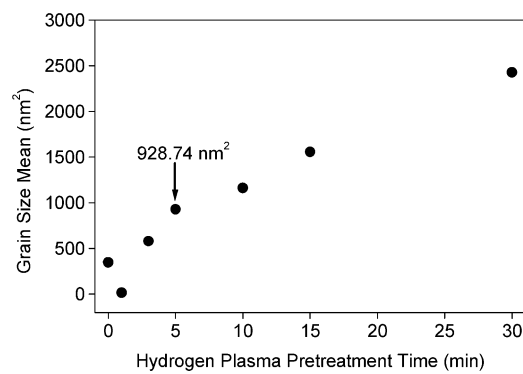
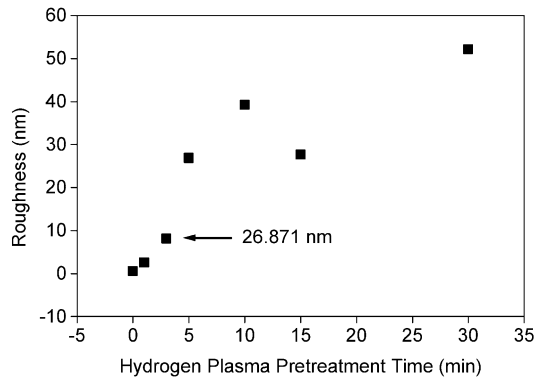


Fig. 2. Surface roughness, average grain size and particle size of  $H_2$  bias-enhanced plasma-pretreated Cr film, obtained for various periods of pre-treatment.

observed by the EDS attached to the TEM, and is the darkest and teardrop-shaped part of this image. A comparison with the SEM photograph in Fig. 3b suggests that the Cr is on top of the CNT.

In most of the existing models of the chemical vapor deposition, the growth of carbon nanotubes are based on the model, first proposed by Baker et al. [11]: the hydrocarbon molecules decompose at the surface of the

catalyst and the carbon atoms dissolve into the metal, forming a solid solution. When this solution becomes supersaturated, C precipitates at the surface of the particle in its stable form as crystalline graphitic layers. Several reported alignment mechanisms were reviewed to explain the possible mechanism in the deposition process performed here. Bower et al. [12] reported that, the alignment is mainly induced by the electrical self-bias field, imposed on the substrate surface from the plasma environment. However, they used heavier ammonia plasma, rather than hydrogen plasma, promoting the establishment of a stronger local field at the surface. They used this fact to explain why others have grown randomly oriented nanotubes in a similar microwave plasma enhanced chemical vapor deposition system

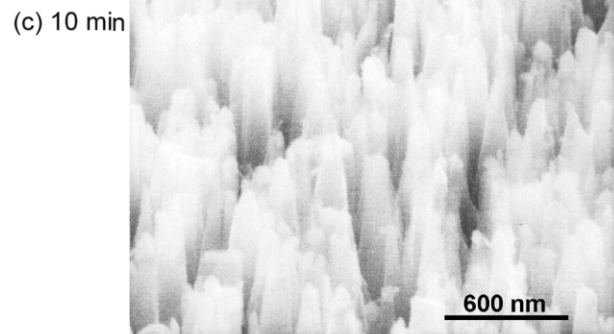
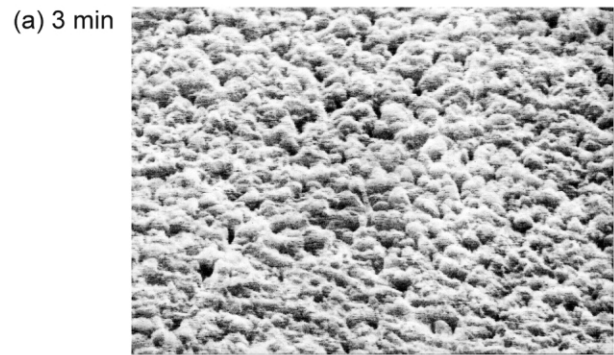


Fig. 3. SEM photographs of samples grown on  $H_2$  plasma-pretreated Cr film pretreated for various periods.

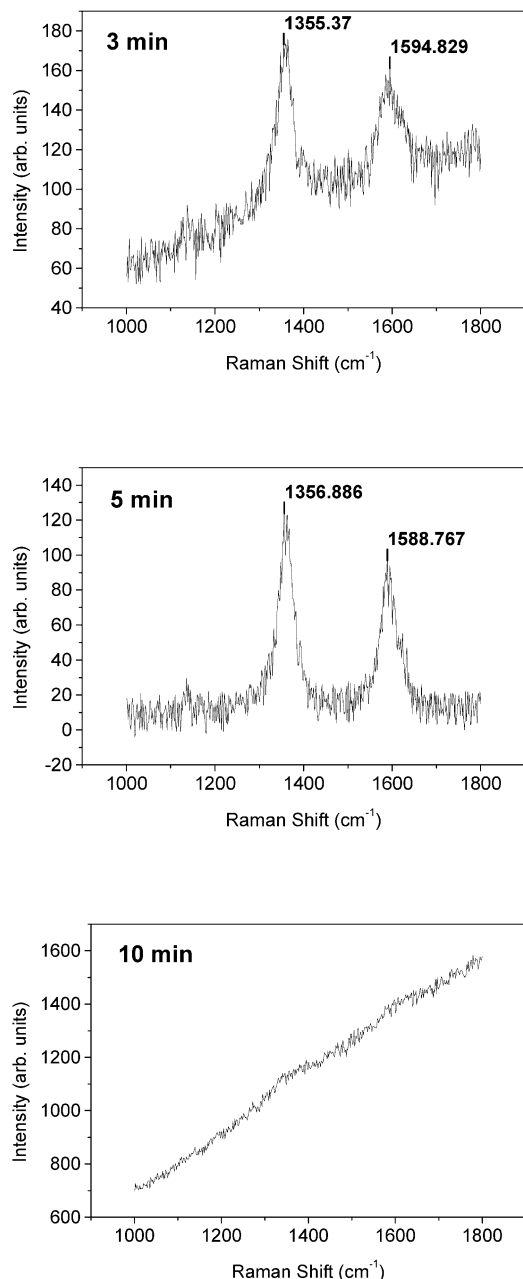


Fig. 4. Raman spectra of samples grown on  $H_2$  plasma-pretreated Cr film pretreated for various periods.

using hydrogen-based plasma [13,14]. A high concentration of hydrogen plasma and a high negative bias applied to the substrate were found to enable the randomly oriented carbon nanotubes to be easily removed by anisotropic etching. Such a mechanism can remove all carbon nanotubes that are not parallel to the hydrogen plasma attracted to the substrate under a negative d.c. bias [8]. Similarly, Murakami et al. [15], developed a process that involved depositing and patterning a nickel-based metal line on a glass substrate, followed by bias-enhanced microwave plasma chemical

vapor deposition to grow well-aligned carbon nanotubes. During nanotube growth, a negative voltage of  $-250$  V was applied to the substrate. Merkulov et al. [16] reported that the crowing effect could assist the alignment of CNTs. However, in this study, it could not be decided that the crowing effect or anisotropic etching which was the main mechanism to assist the alignment of CNTs.

### 3.3. Field emission properties

Field emission properties are obtained using a diode structure. An anode, made of indium tin oxide glass, was separated by  $500 \mu\text{m}$  from the tip of a cathode made of CNTs. The  $I$ - $V$  properties were measured using an electrometer (Keithley 237) and analyzed using the Fowler–Nordheim (F–N) model. Fig. 6 characterizes the VACNTs grown on Cr film pretreated for 5 min. The emission current at an applied voltage of  $1000$  V was  $0.305 \text{ mA/cm}^2$ . The macroscopic turn-on field was  $1.7 \text{ V}/\mu\text{m}$ . In 1928, Fowler and Nordheim proposed the model of field emission from a solid [17]. The F–N model states that the relationship between the emitted current in the local electric field  $F$  and the work function  $\varphi$  is  $I\alpha(F^2/\varphi) \exp(-B\varphi^3/2/F)$ , with  $B=6.83 \times 10^9 (\text{V eV}^{-3/2} \text{ m}^{-1})$ . The local electric field  $F$  is not simply  $V/d$ , which is the macroscopic field obtained when a voltage  $V$  is applied between two electrodes separated by a distance  $d$ . Rather,  $F$  is, in most cases, larger by an enhancement factor  $\beta$ , which reflects the ability of the emitter to amplify the field. The factor  $\beta$  is determined mainly by the geometrical shape of the emitter, and the field at the emitter surface is frequently

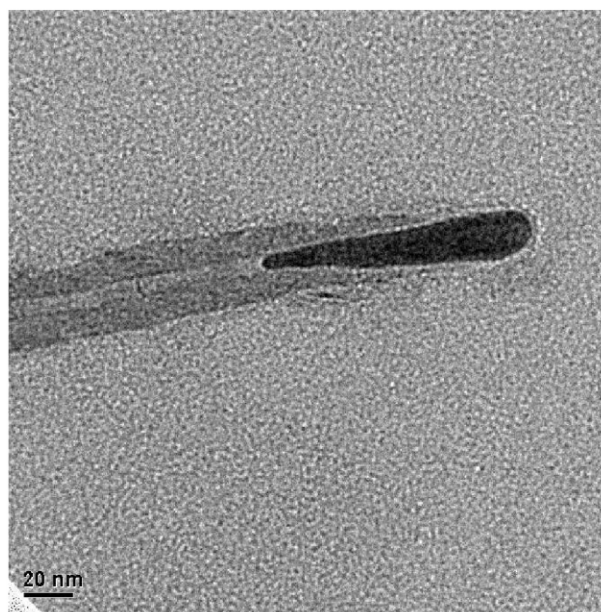


Fig. 5. TEM image of the end section of an individual CNT.

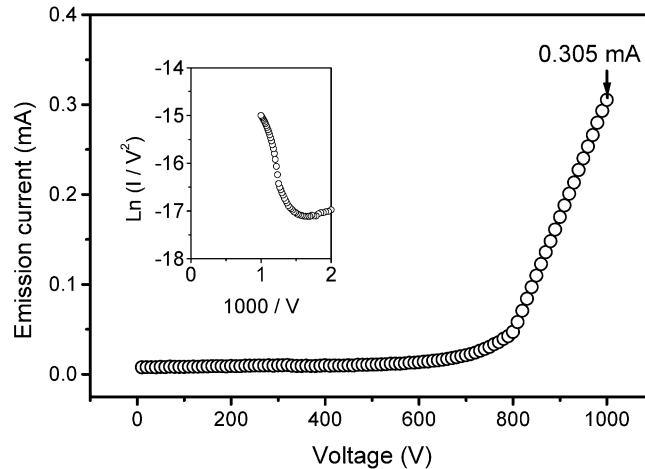


Fig. 6. Emission current against applied voltage, and F–N plot for CNTs.

expressed as  $F = \beta E = \beta V/d$ , where  $E = V/d$  is the macroscopic field. Moreover, literature includes arguments based on values of  $\beta$  that have been determined from the shape of the emitter, and especially from the radius of curvature of the tip,  $R_{\text{tip}}$ . The most basic approximation is  $F \approx V/(kR_{\text{tip}})$ , where  $k$  is a constant that depends on the geometry and is taken to equal 5 for an infinitely long cylindrical emitter [18]. From the aforementioned definition and approximation for  $F$ ,  $\beta = d/(kR_{\text{tip}})$  is obtained. Thus,  $R_{\text{tip}} = 30$  nm yields  $\beta \sim 3000$ .

#### 4. Conclusions

Using  $\text{CH}_4/\text{H}_2$  source gases, VACNTs were grown by microwave plasma chemical vapor deposition on a Cr film, which had been pretreated in bias-enhanced  $\text{H}_2$  plasma for 5 min. Following this pre-treatment, the Cr film provided the catalysts for growing CNTs. The surface roughness, average grain size and particle size of the pretreated Cr film were 26.871 nm, 928.74 nm<sup>2</sup> and 80.409 nm, respectively. The resultant CNTs was vertically aligned; had a notable high-aspect-ratio structure and a diameter of 30 nm. The TEM image indicates that the intrinsic structure is truly that of a CNT and includes teardrop-shaped Cr at the end. The field emission properties of the resultant carbon nanotubes included an emission current of 0.305 mA at 2 V/ $\mu\text{m}$ ; and a turn-on field of 1.7 V/ $\mu\text{m}$ .

#### Acknowledgments

The authors would like to thank the National Science Council of the Republic of China, Taiwan for financially

supporting this work under Contract No. NSC 91-2219-E-009-029.

#### References

- [1] W.A. de Heer, A. Chatelain, D. Ugarte, *Science* 270 (1995) 1190.
- [2] J.M. Bonard, J.P. Salvetat, T. Stockli, L. Forro, *Appl. Phys. Lett.* 75 (1999) 873.
- [3] Z. Yao, C.L. Kane, C. Dekker, *Phys. Rev. Lett.* 84 (2000) 2941.
- [4] E.W. Wong, P.E. Sheehan, C.M. Lieber, *Science* 277 (1997) 1972.
- [5] S. Iijima, *Nature* 354 (1991) 56.
- [6] Z.P. Huang, J.W. Xu, Z.F. Ren, J.H. Wang, M.P. Siegal, P.N. Provencio, *Appl. Phys. Lett.* 73 (1998) 3845.
- [7] M. Okai, T. Muneyyochi, T. Yanguchi, S. Sasaki, *Appl. Phys. Lett.* 77 (2000) 3468.
- [8] S.H. Tsai, C.W. Chao, C.L. Lee, H.C. Shih, *Appl. Phys. Lett.* 74 (1999) 3462.
- [9] R. Andrew, D. Jacques, A.M. Rao, F. Derbyshire, D. Qian, X. Fan, E.C. Dickey, J. Chen, *Chem. Phys. Lett.* 303 (1999) 467.
- [10] Y.Y. Wei, G. Eres, V.I. Merkulov, D.H. Lowndes, *Appl. Phys. Lett.* 78 (2001) 1394.
- [11] R.T.K. Baker, M.A. Barber, P.S. Harris, F.S. Feates, R.J. Waite, *J. Catal.* 26 (1972) 51.
- [12] C. Bower, W. Zhu, S. Jin, O. Zhou, *Appl. Phys. Lett.* 77 (2000) 830.
- [13] L.C. Qin, D. Zhou, A.R. Krauss, D.M. Gruen, *Appl. Phys. Lett.* 72 (1998) 3437.
- [14] O.M. Kuttel, O. Groening, C. Emmenegger, L. Schlapbach, *Appl. Phys. Lett.* 73 (1998) 2113.
- [15] H. Murakami, M. Hirakawa, C. Tanaka, H. Yamakawa, *Appl. Phys. Lett.* 76 (2000) 1776.
- [16] V.I. Merkulov, A.V. Melechko, M.A. Guillorn, D.H. Lowndes, M.L. Simpson, *Appl. Phys. Lett.* 79 (2001) 2970.
- [17] R.H. Fowler, L.W. Nordheim, *Proc. R. Soc. London Ser. A* 119 (1928) 173.
- [18] W.P. Dyke, W.W. Dolan, *Adv. Electron. Electron. Phys.* 8 (1956) 89.